Closing the Loop on Exoskeleton Motor Controllers: Benefits of Regression-Based Open-Loop Control

Greg Orekhov , Jason Luque , and Zachary F. Lerner

Abstract—Lower-limb exoskeletons are widely researched to improve walking performance and mobility. Low-level sensor-less exoskeleton motor control is attractive for consumer applications due to reduced device complexity and cost, but complex and variable transmission system configurations make the development of effective open-loop motor controllers that are responsive to user input challenging. The objective of this study was to develop and validate an open-loop motor control framework resulting in similar or greater performance vs. closed-loop torque control. We used generalized linear regression to develop two open-loop controllers by modeling motor current during exoskeleton-assisted walking; a "complex" model used desired torque and estimated ankle angular velocity as inputs, while a "simple" model used desired torque alone. Five participants walked at 1.0-1.3 m/s on a treadmill with closed-loop and both open-loop controllers providing ankle exoskeleton assistance. Both open-loop current controllers had similar root-mean-squared torque tracking error (p = 0.23) compared to the closed-loop torque-feedback controller. Both openloop controllers had improved relative average torque production (p < 0.001 complex, p = 0.022 simple), lower power consumption (p < 0.001 for both), and reduced operating noise (p = 0.002complex, p < 0.001 simple) over the closed-loop controller. New control models developed for a different ankle exoskeleton configuration showed similar improvements (lower torque error, greater average and peak torque production, lower power consumption) over closed-loop control during over-ground walking. These results demonstrate that our framework can produce open-loop motor controllers that match closed-loop control performance during exoskeleton operation.

Index Terms—Adaptive control, ankle assistance, closed loop, exoskeleton, open loop, statistical modeling.

I. INTRODUCTION

EARABLE exoskeletons provide mechanical assistance to human joints and seek to augment the user's function or task performance [1]. Most exoskeleton research and commercial development has focused on assisting mobility in patient populations with neuromuscular impairment caused by spinal cord injury, stroke or cerebral palsy [2]–[5]. Despite

Manuscript received February 24, 2020; accepted June 23, 2020. Date of publication July 22, 2020; date of current version July 31, 2020. This work was supported in part by NSF Grant #1756029 and NIH Grant #1R15HD099664. (Corresponding author: Zachary F. Lerner.)

Greg Orekhov and Jason Luque are with the Mechanical Engineering Department, Northern Arizona University, Flagstaff, AZ 86011 USA (e-mail: go226@nau.edu; jl2457@nau.edu).

Zachary F. Lerner is with the Mechanical Engineering Department, Northern Arizona University, Flagstaff, AZ 86011 USA, and also with the Department of Orthopedics, The University of Arizona College of Medicine-Phoenix, Phoenix, AZ 85004 USA (e-mail: zachary.lerner@nau.edu).

Digital Object Identifier 10.1109/LRA.2020.3011370

considerable effort, only a few commercially-available devices have measurably improved user performance [6]. Effective high-and low-level control of exoskeleton assistance are two critical components of wearable systems that require special attention, particularly when translating wearable exoskeleton technology from research environments to free-living environments [6]. Research and commercial exoskeleton devices have employed both open- and closed-loop low-level controllers to varying levels of success [7], [8].

Torque sensor-less (i.e., low-level open-loop) exoskeleton actuator control is attractive for research- and commercial-grade devices alike due to lower cost and reduced mechanical and software complexity, which may limit the potential for system instability and bodily harm [9], [10]. However, adequate performance of open-loop controllers depends on proper system and disturbance characterization. Methods involving disturbance observers typically require an inverted mechanical plant model [9], [11], but modeling user-generated exoskeleton disturbances is difficult. Once established, open-loop controllers may require considerably less tuning than closed-loop controllers but, by definition, they may also be less adaptive or responsive. Open-loop characterization of system disturbances can improve exoskeleton performance [11] but the viability of open-loop exoskeleton controllers depends on their responsiveness to user intent across variable walking conditions.

We previously developed a high-level ankle exoskeleton control scheme that provided adaptive assistance proportional to the biological joint moment [13]. We subsequently demonstrated the ability of this controller, implemented on an untethered cable-actuated ankle exoskeleton, to improve over-ground walking economy in individuals with cerebral palsy [4]. In our prior research, the control signal from this high-level algorithm was prescribed via a closed-loop proportional-derivative (PD) torque-feedback controller. While the high-level algorithm nicely adapted the torque set points to variable ankle demand, we observed high battery power consumption, loud operating noise, and occasional difficulty with tracking peak torque values that were within the mechanical capabilities of the device. These findings, coupled with a desire for a simpler, more reliable system, motivated a renewed investigation into low-level exoskeleton control. Surprisingly, we were unable to find any published work that compared the performance of open-loop vs. closed-loop control during exoskeleton-assisted walking trials. Accurate analytical models for cable-driven robot control are difficult to develop because cable routing and tension affect friction compensation [12]. For lower-extremity exoskeletons

2377-3766 © 2020 IEEE. Personal use is permitted, but republication/redistribution requires IEEE permission. See https://www.ieee.org/publications/rights/index.html for more information.

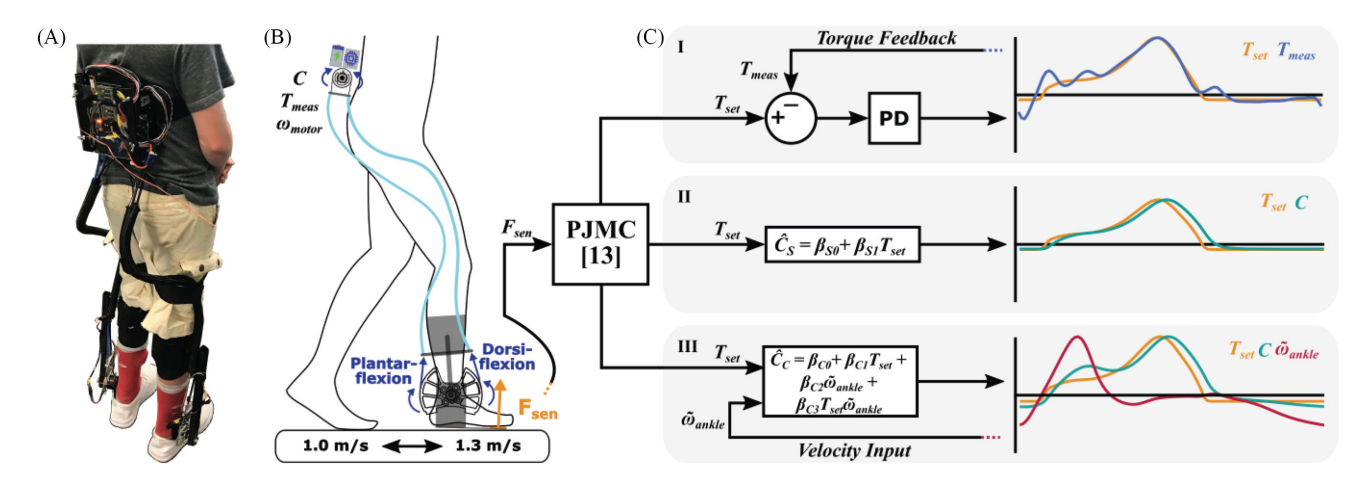


Fig. 1. Mechanical and control system overview. (A) A user wearing our bilateral ankle exoskeleton. (B) Simple visualization of exoskeleton function and experimental setup utilizing a treadmill at typical adult walking speeds [22]–[24]. Proportional joint moment control (PJMC) defines the assistance profile T_{set} from the instantaneous force reading F_{sen} [13]. A torque sensor at the ankle measures applied torque T_{meas} . On-board sensing and calculations yield motor current C and estimate ankle angular velocity $\tilde{\omega}_{ankle}$ from measured motor velocity ω_{motor} . (C) Simplified block diagrams of closed- and open-loop control schemes. Closed-loop torque control (I) minimizes error between T_{meas} and T_{set} using a PD controller. Simple open-loop current control (II) predicts a current setpoint \hat{C}_{C} from T_{set} only. Complex open-loop current control (III) predicts a current setpoint \hat{C}_{C} from T_{set} , real-time velocity input $\tilde{\omega}_{ankle}$, and the interaction of the two signals. β_{i} are coefficients determined from generalized linear regression and can be found in equations 4-7 of the text. Plots of experimental data demonstrate the variability in control objectives, input, and output signals for the three control modes.

designed to conform to each user, variable cable routing that changes over the gait cycle and which is difficult to quantify poses a considerable challenge for generalizing characterization of analytical model parameters.

The objective of this study was to develop an effective empirical modeling framework for generating open-loop motor control schemes of cable-driven ankle exoskeletons that meet or exceed the performance of closed-loop torque-feedback control. We utilized regression-based system modeling to establish relationships between delivered torque and prescribed motor current during the robot's use case – walking at variable speeds. Our primary hypothesis was that an appropriately modeled open-loop current controller could meet and potentially exceed the performance of closed-loop torque-feedback control. Our secondary hypothesis was that inclusion of estimated ankle velocity as a model input would increase the responsiveness and therefore performance of open-loop motor control. We assessed the performance of two regression-based open-loop motor current controllers (velocity- & torque-input and just torque-input) by comparing torque tracking error, average joint torque, power consumption, and noise production to our standard closed-loop torque-feedback controller during exoskeleton-assisted treadmill walking at moderate speeds. To the best of our knowledge, this is the first study to use regression-based empirical methods to model open-loop exoskeleton dynamics in functional use cases.

II. METHODS

A. Ankle Exoskeleton and High-Level Control Algorithm

For this study, we used a battery-powered and wireless ankle exoskeleton designed to provide both plantarflexion (PFX) and dorsiflexion (DFX) assistance [4], [14]. To summarize exoskeleton design, which has been reported in extensive detail previously, brushless DC motors (EC4-Pole 30 200W, Maxon)

worn around the waist actuated Bowden cables that subsequently rotated a pulley at the ankle joint (Fig. 1AB). The pulley was mounted to a carbon fiber footplate that rotated relative to a carbon fiber calf cuff. A torque sensor between the pulley and footplate measured applied torque and, in the case of closed-loop control, provided feedback to a control unit. The control unit included a microprocessor, motor drivers, signal processing chips, and Bluetooth module. Force-sensitive resistors (FSRs) on the footplate detected gait events and informed a simple state machine to appropriately shift between PFX and DFX assistance during the stance and swing phases of walking (Fig. 1B). A 5-sample moving average filtered torque sensor and FSR analog readings.

The exoskeleton assistance profile was controlled by an instantaneously-adaptive Proportional Joint Moment Controller (PJMC) [13]. PJMC prescribed the desired torque (T_{set}) as in equation (1):

$$T_{set} = T_0 \frac{F_{sen}}{F_{ref}} \tag{1}$$

where F_{sen} was the real-time FSR reading and F_{ref} was the average peak FSR reading during a baseline calibration. The instantaneous sensor force ratio scaled the desired peak torque setpoint T_0 (e.g., 15 Nm) so that it adapted assistance based on the ankle demand across variable walking conditions [13]. The PJMC controller was calibrated once during steady-state walking conditions so that any change in speed was reflected in the real-time FSR reading F_{sen} , which automatically adjusted the desired torque profile [13].

In the case of closed-loop control, a PD controller tracked T_{set} based on the ankle torque (T_{meas}) measured from the embedded torque sensor (Fig. 1C, I). The PD gains for this controller were carefully tuned to track the desired PFX torque while limiting resonance (i.e., oscillation amplitude amplification) and overshoot. This closed-loop controller and these PD gains were

used in previous studies that demonstrated clinically significant improvements in joint kinematics, positive ankle joint power, and metabolic cost of transport in people with cerebral palsy [4], [15] – outcomes that depended on an appropriately tuned control system.

B. Open-Loop System Modeling for Low-Level Control

Developing an open-loop motor controller capable of accurately prescribing the high-level adaptive assistance torque from PJMC required precisely characterizing exoskeleton interaction with the user during walking. Instead of attempting to develop and validate an analytical model of the exoskeleton system dynamics coupled with complex human interaction, we sought to develop an empirical model to characterize the system experimentally. We first used a basic open-loop current controller to collect the experimental data for empirically predicting motor current as a function of ankle torque alone or both ankle torque and motor velocity during walk across a range of speeds and PFX assistance levels. The basic open-loop current controller specified motor current (C_{set}) as in equation (2):

$$C_{set} = T_{set} \left(\tau_m R_{gb} R_p \varepsilon_{mgb} \right)^{-1} \tag{2}$$

where the torque setpoint (T_{set}) was divided by the motor torque constant (τ_m) , gearbox and pulley gear ratios $(R_{gb}$ and R_p , respectively) and motor and gearbox efficiencies (ε_{mgb}) . The gearbox and pulley ratios were 103:1 and 2.3:1, respectively. The microcontroller recorded the motor current (C) and the average motor angular velocity (ω_{motor}) from the motor drivers (ESCON 50/8, Maxon). Maxon motors use hall sensors to detect shaft velocity. Ankle angular velocity $(\tilde{\omega}_{ankle})$ was estimated using motor and exoskeleton gear ratios assuming no transmission losses, as in equation (3):

$$\tilde{\omega}_{ankle} = \omega_{motor} (R_{gb} R_p)^{-1}.$$
 (3)

Collecting data during functional use cases ensured that system characteristics, such as energy lost due to friction, and human disturbances, such as walking speed and assistance profile variability, were sufficiently captured and subsequently modeled. Motivated by the critical role of positive mechanical ankle joint power for efficient locomotion [14], [16]–[18] and based on the rationale that DC motors operate with an inverse relationship between motor torque production and output velocity [19], we hypothesized that motor current could be accurately modeled using the measured torque (T_{meas}) and the estimated ankle angular velocity $(\tilde{\omega}_{ankle})$.

We developed a generalized linear model (GLM) of motor current in MATLAB using T_{meas} and $\tilde{\omega}_{ankle}$ as inputs assuming normal distributions and a unity link function [20]. Positive $\tilde{\omega}_{ankle}$ values correspond to ankle PFX. All coefficients of the fitted model, including the interaction of T_{meas} and $\tilde{\omega}_{ankle}$, were significant at 95% confidence. The complex current model (\hat{C}_C) coefficients are summarized below (Eq. 4).

$$\hat{C}_C = -0.124 + 0.282 T_{meas} + 0.0578 \,\tilde{\omega}_{ankle} + 0.002 T_{meas} \,\tilde{\omega}_{ankle}$$
(4)

TABLE I PARTICIPANT CHARACTERISTICS

User	Age [Years]	Sex	Mass [kg]	Experience	Controller Preference
P1	30	F	59.4	Advanced	Simple open
P2	27	M	69.5	Beginner	Closed
Р3	25	M	86.6	Advanced	Complex open
P4	21	F	77.2	Beginner	Closed
P5	31	M	65.8	Advanced	Complex open
SP1	25	M	81.6	Advanced	Simple open

Experience: Familiarity walking in the exoskeleton prior to data collection. Preference of controller was surveyed after data collection. SP1 completed the over-ground experiment.

We also developed a simple motor current model (\hat{C}_S) with only T_{meas} as an input (Eq. 5) for the purpose of testing our secondary hypothesis that ankle velocity is important for modeling exoskeleton responsiveness.

$$\hat{C}_S = -0.055 + 0.291 T_{meas} \tag{5}$$

To employ the regression equations for open-loop control, we replaced T_{meas} with T_{set} such that both models predict current using the adaptive desired assistance profile defined by PJMC (Fig. 1C).

The parameter coefficients of both GLMs can be interpreted to make informed predictions about exoskeleton performance when using these regression-based open-loop current controllers. Since both models are dominated by the torque term, the predicted motor current profile will closely match the desired torque assistance profile. We also expect that the complex (velocity- & torque-input) open-loop controller will be more responsive than the simple (just torque-input) open-loop controller because the velocity term in Eq. 4 will increase current in response to high ankle angular velocity (Fig. 1C), such as during heel strike and toe-off regions of gait. Furthermore, the interaction term in the complex model represents mechanical ankle joint power; this term likely favorably increases current production when torque and ankle angular velocity have the same direction.

C. Exoskeleton Motor Controller Comparison Experiment

We evaluated the low-level exoskeleton motor controllers during a treadmill walking experiment approved by Northern Arizona University's Institutional Review Board under protocol #986744. Five unimpaired individuals participated in the study (Table I). Written informed consent for each participant was obtained prior to enrollment. Exclusion criteria included any health condition that could affect walking ability or participant safety. An operator controlled the treadmill and exoskeleton through a MATLAB graphical user interface. Participants wore the exoskeleton and walked on a treadmill at 1.0 m/s for PJMC baseline calibration; the same participant-specific FSR sensor calibration was used for all trials. All participants were prescribed 0.25 Nm/kg peak PFX torque assistance.

Participants walked with closed-loop torque control, simple (torque-input) open-loop current control, and complex (velocity-& torque-input) open-loop current control in single-blind randomized order. Participants were told to walk normally prior to the experiment. No coaching or instructions were provided during walking trials. Treadmill speed was set to 1.0 m/s, then 1.3 m/s, and back to 1.0 m/s; these speeds are within the typical ranges for children and adults with cerebral palsy [4], [21], stroke survivors [2], and unimpaired adults [22]– [24]. The acceleration/deceleration between speeds was set to 0.02 m/s². The time spent at each steady-state speed interval was 3 minutes.

We recorded the desired torque set point (T_{set}) , measured torque (T_{meas}) , motor current (C), and motor angular velocity (ω_{motor}) . Exoskeleton state transitions separated signals into PFX and DFX regions corresponding to stance and swing phases of gait, respectively [4]. Controller performance analysis and assessment, performed across the entire stance phase, was completed using MATLAB.

Primary controller performance outcome measures included deviance from the desired control signal, overall torque and power generation capacity, battery power consumption, and noise. We calculated root-mean-squared error (RMSE) between T_{set} and T_{meas} to quantify assistance profile tracking performance. Average stance phase measured torque \bar{T}_{meas} was calculated and normalized by corresponding average demand torque \bar{T}_{set} to assess average torque capacity and overall assistance potential. Similarly, peak torque tracking was quantified by the ratio of maximum demanded torque T_{set} and corresponding measured torque T_{meas} .

Battery power consumption was calculated by numerically integrating motor current C with respect to time and is reported in typical units of battery capacity in Ah. We normalized power consumption by \bar{T}_{meas} to evaluate power use relative to torque produced. Noise levels were calculated by averaging measured sound recordings over the course of each trial.

The demand assistance profile T_{set} is generated in real-time to instantaneously adapt the torque profile to variations in speed and terrain [13]. Additionally, angular velocity is an important contributor to ankle power [16], [17] and a controller must be able to provide torque assistance without limiting joint range of motion. To assess controller kinematic adaptability, motor peak PFX (toe-off) angular velocities for each stance phase were also collected and averaged.

D. Framework Verification Experiment

To verify the effectiveness of our controller design framework and demonstrate utility beyond treadmill walking, we recruited an additional participant SP1 (Table I) to perform over-ground exoskeleton walking experiments. The same general protocol was followed to build new open-loop GLMs and compare closed-loop and open-loop controllers. We purposefully used a different exoskeleton mechanical assembly, including different motors (EC4-Pole 22 120W, Maxon), gearbox and pulley ratios (123:1 and 2.9:1, respectively), and actuation cable lengths than the exoskeleton used for treadmill experiments. The resulting complex and simple models for this exoskeleton are summarized

in equations (6) and (7), respectively. As before, we replaced T_{meas} with T_{set} when implementing the open-loop controllers (Fig. 1C, II and III).

$$\hat{C}_C = 0.343 T_{meas} + 0.0236 \tilde{\omega}_{ankle}$$

$$+ 0.004 T_{meas} \tilde{\omega}_{ankle}$$
(6)

$$\hat{C}_S = 0.373 T_{meas} \tag{7}$$

SP1 walked one lap around a 60 m track with 0.25 Nm/kg PFX assistance and 1 Nm DFX assistance for each controller. Additionally, SP1 walked one lap with no assistance or resistance using the closed-loop controller (i.e., zero-torque control [14]) to capture motor behavior under minimal-load conditions. All trials utilized the same PJMC baseline calibration. During each lap, we captured T_{set} , T_{meas} , C, and ω_{motor} . Each lap contained between 37 and 38 complete strides and each stride was treated as an individual observation. Average walking speed, estimated from individual lap speeds, was 1.25 ± 0.03 m/s. Similar data processing as for the treadmill experiment was used to calculate performance metrics. We also compared motor velocity during toe-off between the three controllers and the closed-loop zero-torque control trial.

E. Statistics

Samples from each walking speed were pooled together for statistical analysis to collectively quantify performance across all experimental conditions. The typical number of strides (mean \pm standard deviation) averaged and analyzed was 311.8 \pm 14.1 strides for closed-loop control, 312.2 \pm 9.1 strides for simple open-loop control, and 313.4 \pm 14.2 strides for complex open-loop control. All experimental data were tested for outliers in MATLAB within and across participants. Outliers 1.5 times the interquartile range past the first or third quartiles for the data set were removed from further analysis. Each performance metric was treated as an independent set of samples when testing for outliers. When an outlier was removed, corresponding observations were also removed from each control mode within the specific metric to maintain a balanced study design. Oneway repeated measures analyses of variance (ANOVAs) were used to detect differences in performance metrics between the closed-loop torque control, simple open-loop current control, and complex open-loop current control schemes. Significantly different means detected by ANOVAs were further analyzed with post-hoc Tukey tests with corrections for multiple comparisons. All statistical analyses were performed at 95% confidence.

III. RESULTS

During the main controller comparison experiment, all three controllers had statistically similar torque RMSE during stance phase assistance (p = 0.23, Fig. 2A). Both open-loop controllers had a significantly improved average relative torque ratios (T_{meas}/T_{set}) compared to the closed-loop controller (p = 0.022 for the simple model, p < 0.001 for the complex model, Fig. 2B); average torque ratio was similar between the two open-loop controllers (p = 0.46). Both open-loop controllers had a similar peak relative torque ratio vs. the closed-loop controller (p = 0.21).

Exoskeleton Motor Controller Comparison Experiment

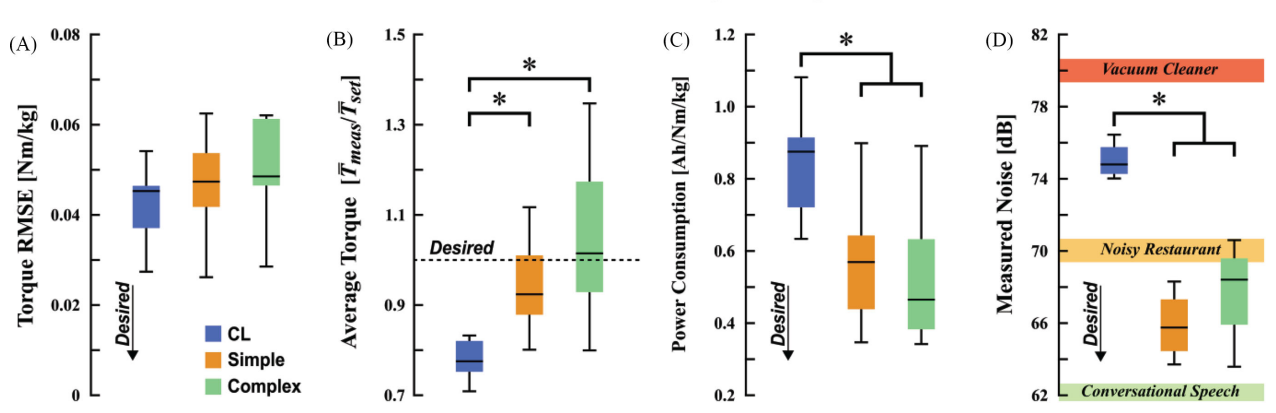


Fig. 2. Summary of treadmill controller performance metrics and statistical analyses. Minimum, first quartile, median, third quartile, and maximum values shown. * indicates a significant difference between control modes at 95% confidence. Closed-loop (CL), simple open-loop, and complex open-loop controller results shown. (A) Total stance phase exoskeleton torque root-mean-square error (RMSE). (B) Measured torque averaged across each stance phase, \bar{T}_{meas} , normalized by the average desired torque of the same step, \bar{T}_{set} . The ratio of measured to desired torque quantifies controller overshoot and general system torque capacity. (C) Power consumption normalized by average measured torque \bar{T}_{meas} . (D) Measured exoskeleton noise during operation.

Framework Verification Experiment

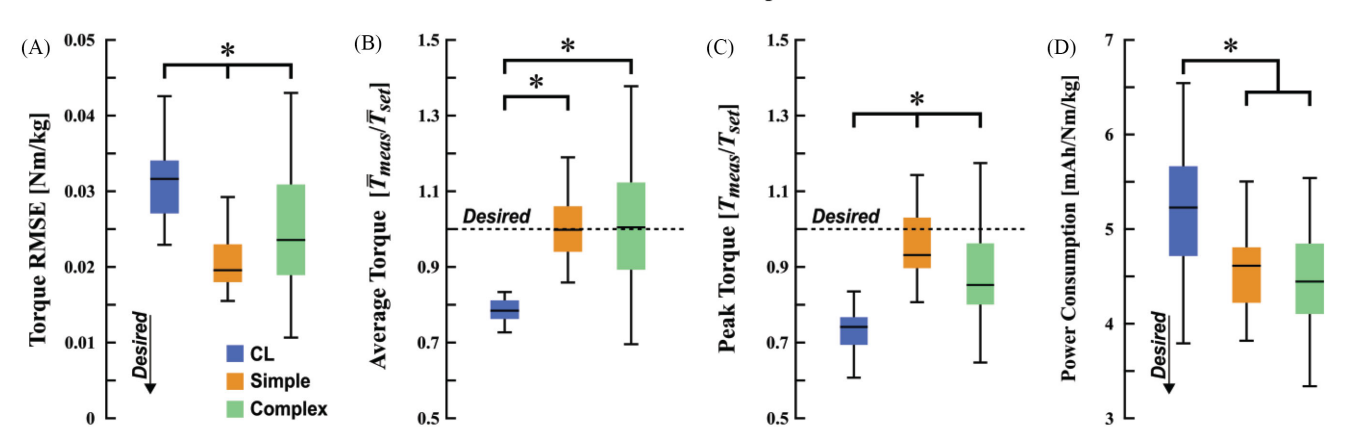


Fig. 3. Summary of over-ground controller performance metrics and statistical analyses. Minimum, first quartile, median, third quartile, and maximum values shown. * indicates a significant difference between control modes at 95% confidence. Closed-loop (CL), simple open-loop, and complex open-loop controller results shown. (A) Stance phase exoskeleton torque root-mean-square error (RMSE) per step. (B) Measured torque averaged across each stance phase, \bar{T}_{meas} , normalized by the average desired torque of the same step, \bar{T}_{set} . The ratio of measured to desired torque quantifies controller overshoot and general system torque capacity. (C) The ratio of measured to peak demanded torque T_{meas}/T_{set} quantifies peak torque tracking and capacity. (D) Power consumption per step normalized by the average measured torque of that step \bar{T}_{meas} .

The simple and complex open-loop controllers had lower power consumption (p < 0.001 for both, Fig. 2C) and noise generation (p < 0.001 for the simple controller, p = 0.002 for the complex controller, Fig. 2D) compared to the closed-loop controller. Participants were asked to state their controller preference (Table I) and provide a qualitative comparison of the three control modes.

During the framework verification experiment, all three controllers had significantly different torque RMSE during stance (Fig. 3A, 4A). Closed-loop torque control had the highest torque RMSE (p < 0.001 vs. both). Simple open-loop control had the lowest torque RMSE (p = 0.010 vs. complex open-loop). Both open-loop controllers had significantly improved average relative torque ratios compared to the closed-loop controller (p < 0.001 for both, Fig. 3B). All three controllers had significantly different peak torque ratios (p < 0.001 closed-loop

vs. both open-loop controllers, p=0.009 simple vs. complex open-loop, Fig. 3C); simple open-loop had the highest ratio while closed-loop control had the lowest. Closed-loop control had the highest power consumption per step (p<0.001 vs. both open-loop controllers, Fig. 3D); the open-loop controllers had similar consumption (p=0.74).

IV. DISCUSSION

We accept our primary hypothesis that an appropriately modeled open-loop current controller can meet or exceed the performance of closed-loop torque-feedback control for providing adaptive cable-actuated ankle exoskeleton assistance during walking. Specifically, both open-loop current controllers had similar torque profile RMSE and peak relative torque ratios

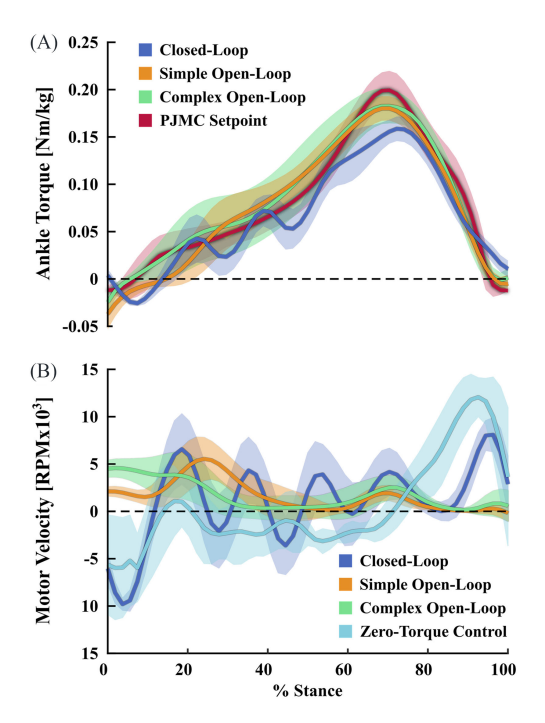


Fig. 4. Stance phase ankle torque (A) and motor velocity (B) profiles during over-ground walking. Lines designate the mean profile and shaded regions show standard deviations.

vs. the closed-loop torque controller, and both open-loop controllers also had greater average measured to demanded torque, better (lower) battery power consumption relative to torque output, and quieter function than the closed-loop controller during treadmill walking (Fig. 2). Both open-loop controllers adapted well to changes in walking speed and torque demand, consistently producing good profile tracking. We accomplished this by modeling human-robot interactions using generalized linear regression during functional use cases, thereby capturing exoskeleton and human dynamics including inefficiencies due to friction and transmission losses. This empirical method was quick (< 15 minutes) and effective in modeling two different cable-actuated exoskeletons. The framework verification experiment corroborated the treadmill results and provided evidence that our proposed empirical method for developing open-loop controllers can be generalized to other cable-actuated exoskeletons. Though promising, the results should be interpreted with care as this preliminary study involved only a few unimpaired participants under controlled conditions. Future work will expand the quantity and variety of participants and walking scenarios.

We asked participants to identify their preferred controller to assess whether perception matched the quantitative performance results. Controller preference was varied: two participants preferred the closed-loop torque controller, two preferred the complex model open-loop controller, and one preferred the simple model open-loop controller (Table I). The supplemental participant also preferred the simple open-loop controller, splitting preference evenly among the three controllers. The two participants that preferred closed-loop torque control stated that they liked the responsiveness compared to the open-loop controllers that felt "stiffer" and "less responsive". On the other

hand, most participants commented that open-loop control felt more "consistent" and "assistive", particularly regarding peak torque, which supported the results showing improved relative torque production when walking with open-loop controllers.

We are unable to prove or disprove our secondary hypothesis that the inclusion of motor velocity as a model input would result in improved open-loop controller performance. There were no statistically significant differences between the simple and complex open-loop controller performance metrics during the main treadmill experiment (Fig. 2), while the simple open-loop controller had lower torque RMSE vs. the complex controller during the framework verification experiment (Fig. 3). Prompted by these results, we completed a post-hoc bench-top analysis to verify our ability to estimate ankle velocity from motor velocity (i.e., Eq. (3)). We observed considerable compliance in the ankle joint's angular position ($\sim 15^{\circ}$) when the motors were stalled, confirming our suspicion that motor angular velocity cannot be used to accurately estimate ankle angular velocity due to mechanical elasticity and deformation of the Bowden cable transmission system at high torque. While including scaled motor velocity (i.e., estimated ankle velocity) as a model input was ineffective at improving open-loop motor control, future work should evaluate the use of an angular velocity sensor in-line with the ankle joint.

We initially planned to analyze peak ankle angular toe-off velocity and compare PFX power production for each controller. Peak ankle joint mechanical power typically occurs during the late stance phase of walking when the ankle produces large plantar-flexor angular velocity and moment during push-off [16], [18], [25]. User comments that the open-loop controllers felt "stiffer" encouraged a closer look at motor behavior during assistance. We discovered that all three controllers significantly underestimated peak biological ankle velocity during toe-off [26]. This was likely the result of series elasticity across the transmission system and ankle assembly, but also the inverse relationship between torque production and angular velocity for DC motors [19]. For example, the closed-loop controller had reduced toe-off velocities when providing assistance vs. when operating in zero-torque control (p < 0.001, Figs. 4, 5B).

Open-loop control had lower toe-off velocity than closed-loop control, which may have contributed to user perception of "stiffness" but also improved torque production efficiency (Figs. 4, 5). The open-loop controllers may have utilized transmission friction and elastic deformation of carbon fiber exoskeleton components to "build" torque during early-mid stance that subsequently was "released" during toe-off, requiring less motor power. User perception was that assistance was much stronger with open- vs. closed-loop control. We plan to conduct a more-detailed biomechanical analysis using motion capture and explore methods for improving responsiveness in the open-loop controllers; a direct measurement of ankle joint velocity may improve the complex (velocity- & torque-input) controller performance.

Future work should quantify the effects of closed-loop vs. open-loop motor controllers upon human gait mechanics, energetics, and muscle control, particularly over an extended acclimation period with the exoskeleton. Several previous studies demonstrated clinically significant improvements in

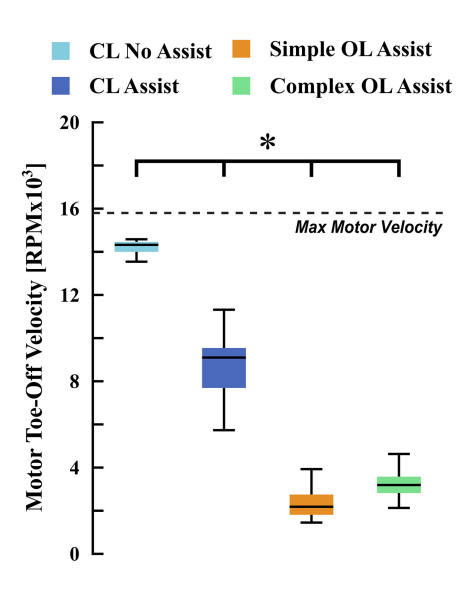


Fig. 5. Comparison of motor toe-off velocity during over-ground walking. The open-loop (OL) controllers and the closed-loop (CL) controller with assistance were all significantly different from each other and from the no-load velocity.

joint kinematics, positive ankle power, muscle activity, and metabolic cost of transport in impaired populations using the closed-loop torque-feedback controller [4], [14], [15]. There is evidence that humans entrain (i.e., adapt biomechanics) to the frequency of external stimuli such as mechanical perturbations [27], [28]. While torque tracking was similar between open- and closed-loop motor control, user perception of "more consistent" assistance for open-loop control suggests that it may be more effective than closed-loop controllers at improving gait mechanics in individuals with neuromuscular impairment as the rhythmic nature of open-loop control may encourage a consistent step cadence and a reduction in muscle firing pattern variability.

Open-loop control may be particularly attractive for commercialization because it produced significantly reduced audible noise and had more efficient torque production. The open-loop controllers averaged 127% of the closed-loop average torque output with 64% of the battery consumption and only 89% of the audible decibel readings (Fig. 6). The 11% reduction in decibel measurement, or around 8 dB, means that the open-loop controllers were nearly half as loud as the closed-loop controller due to the logarithmic scale; noise level went from close to that of a vacuum cleaner for closed-loop control to close to that of conversational speech for open-loop control.

In summary, the results of this study show that a simple empirical modeling framework can be effective for developing sensor-less motor controllers for cable-actuated robotic exoskeletons. Both simple (torque-input only) and complex (velocity- and torque-input) open-loop controllers matched or exceeded the torque tracking and capacity of our finely-tuned closed-loop torque-feedback controller with significantly lower noise and power consumption during walking (Figs. 2, 3, 5A, and 6). It remains unclear whether velocity input is beneficial for open-loop controller performance, though the high variability in performance of the complex controller suggests better sensitivity to different gait patterns than the simple controller. Low-level

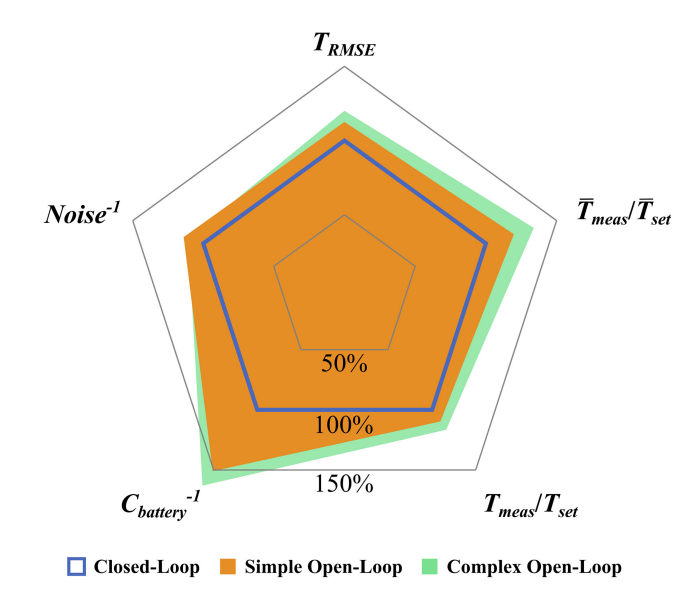


Fig. 6. A radar plot of the primary controller performance metrics. Treadmill results from the simple and complex open-loop controllers are reported as a percentage of the results from closed-loop control indicated with a blue dashed pentagon. The open-loop controllers had reduced noise and power consumption $C_{battery}$, increased average stance torque ratio $\bar{T}_{meas}/\bar{T}_{set}$, and similar torque tracking T_{RMSE} and peak stance torque ratio T_{meas}/T_{set} .

open-loop exoskeleton motor controllers hold potential to improve exoskeleton performance and reduce cost, weight, and complexity by eliminating the need for torque-feedback sensors. The resulting improvements in power consumption and noise generation may facilitate commercialization, long-term intervention studies, and out-of-lab use. Future work will address the limitation of estimating ankle velocity using motor hall sensors and elucidate exoskeleton-user interaction.

REFERENCES

- L. M. Mooney and H. M. Herr, "Biomechanical walking mechanisms underlying the metabolic reduction caused by an autonomous exoskeleton," J. Neuroeng. Rehabil., vol. 13, no. 4, 2016, doi: 10.1186/s12984-016-0111-3.
- [2] L. N. Awad et al., "A soft robotic exosuit improves walking in patients after stroke," Sci. Transl. Med., vol. 9, no. 400, 2017, Art. no. eaai9084.
- [3] E. M. McCain et al., "Mechanics and energetics of post-stroke walking aided by a powered ankle exoskeleton with speed-adaptive myoelectric control," J. Neuroeng. Rehabil., vol. 16, no. 57, 2019, doi: 10.1186/s12984-019-0523-y.
- [4] G. Orekhov, Y. Fang, J. Luque, and Z. F. Lerner, "Ankle exoskeleton assistance can improve over-ground walking economy in individuals with cerebral palsy," *IEEE Trans. Neural Syst. Rehabil. Eng.*, vol. 28, no. 2, pp. 461–467, Jan. 2020.
- [5] Z. F. Lerner, D. L. Damiano, and T. C. Bulea, "A lower-extremity exoskeleton improves knee extension in children with crouch gait from cerebral palsy," Sci. Transl. Med., vol. 9, no. 404, 2017, Art. no. eaam9145.
- [6] A. J. Young and D. P. Ferris, "State of the art and future directions for lower limb robotic exoskeletons," *IEEE Trans. Neural Syst. Rehabil. Eng.*, vol. 25, no. 2, pp. 171–182, Feb. 2017.
- [7] L. M. Mooney, E. J. Rouse, and H. M. Herr, "Autonomous exoskeleton reduces metabolic cost of walking," in *Proc. 36th Ann. Int. Conf. IEEE Eng. Medicine Bio. Soc.*, 2014, pp. 3065–3068.
- [8] I. Kang, H. Hsu, and A. Young, "The effect of hip assistance levels on human energetic cost using robotic hip exoskeletons," *IEEE Robot. Autom. Lett.*, vol. 4, no. 2, pp. 430–437, Apr. 2019.
- [9] T. Murakam, F. Yu, and K. Ohnishi, "Torque sensorless control in multidegree-of-freedom manipulator," *IEEE Trans. Ind. Electron.*, vol. 40, no. 2, pp. 259–265, Apr. 1993.

- [10] N. Vitiello, T. Lenzi, S. M. M. De Rossi, S. Roccella, and M. C. Carrozza, "A sensorless torque control for antagonistic driven compliant joints," *Mechatronics*, vol. 20, no. 3, pp. 355–367, 2010.
- [11] B. Ugurlu, M. Nishimura, K. Hyodo, M. Kawanishi, and T. Narikiyo, "A framework for sensorless torque estimation and control in wearable exoskeletons," in *Proc. Int. Workshop Adv. Motion Control*, 2012, pp. 1–7.
- [12] U. Jeong and K. J. Cho, "Feedforward friction compensation of Bowdencable transmission via loop routing," in *Proc. IEEE Int. Conf. Intell. Robots Syst.*, Dec. 2015, pp. 5948–5953.
- [13] G. M. Gasparri, J. Luque, and Z. F. Lerner, "Proportional joint-moment control for instantaneously adaptive Ankle exoskeleton assistance," *IEEE Trans. Neural Syst. Rehabil. Eng.*, vol. 27, no. 4, pp. 751–759, Apr. 2019.
- [14] Z. F. Lerner et al., "An untethered ankle exoskeleton improves walking economy in a pilot study of individuals with cerebral palsy," *IEEE Trans. Neural Syst. Rehabil. Eng.*, vol. 26, no. 10, pp. 1985–1993, Sep. 2018.
- [15] Z. F. Lerner, T. A. Harvey, and J. L. Lawson, "A battery-powered ankle exoskeleton improves gait mechanics in a feasibility study of individuals with cerebral palsy," *Ann. Biomed. Eng.*, vol. 47, no. 6, pp. 1345–1356, 2019
- [16] D. J. Farris and G. S. Sawicki, "The mechanics and energetics of human walking and running: A joint level perspective," *J. Roy. Soc. Interface*, vol. 9, no. 66, pp. 110–118, 2012.
- [17] G. S. Sawicki and D. P. Ferris, "Mechanics and energetics of level walking with powered ankle exoskeletons," *J. Exp. Biol.*, vol. 211, no. 9, pp. 1402–1413, 2008.
- [18] M. B. Wiggin, G. S. Sawicki, and S. H. Collins, "An exoskeleton using controlled energy storage and release to aid ankle propulsion," in *Proc. IEEE Int. Conf. Rehabil. Robot.*, 2011, Art. no. 5975342.

- [19] C. J. Bishop and R. H. Bishop, Section 20.2 "Electrical machines," in The Mechatronics Handbook. Boca Raton, FL, USA: CRC Press, 2002, pp. 557–565.
- [20] M. J. Campbell and A. J. Dobson, "An introduction to generalized linear models," *Biometrics*, vol. 47, no. 1, pp. 347, 1991.
- [21] M. F. Abel and D. L. Damiano, "Strategies for increasing walking speed in diplegic cerebral palsy," *J. Pediatr. Orthop.*, vol. 16, no. 6, pp. 753–758, 1996.
- [22] M. J. Chung and M. J. J. Wang, "The change of gait parameters during walking at different percentage of preferred walking speed for healthy adults aged 20-60 years," *Gait Posture*, vol. 31, no. 1, pp. 131–135, 2010
- [23] H. G. Kang and J. B. Dingwell, "Separating the effects of age and walking speed on gait variability," *Gait Posture*, vol. 27, no. 4, pp. 572–577, 2008.
- [24] J. Zhang et al., "Human-in-the-loop optimization of exoskeleton assistance during walking," Sci. (80-.)., vol. 356, no. 6344, pp. 1280–1283, 2017.
- [25] A. Hreljac, "Determinants of the gait transition speed during human locomotion: Kinematic factors," *J. Biomech.*, vol. 28, no. 6, pp. 669–677, 1995
- [26] K. P. Granata, M. F. Abel, and D. L. Damiano, "Joint angular velocity in spastic gait and the influence of muscle- tendon lengthening," *J. Bone Joint Surg. - Ser. A*, vol. 82, no. 2, pp. 174–186, 2000.
- [27] J. Ahn and N. Hogan, "Walking is not like reaching: Evidence from periodic mechanical perturbations," *PLoS One*, vol. 7, no. 3, 2012, doi: 10.1371/journal.pone.0031767.
- [28] N. Hogan and D. Sternad, "Dynamic primitives in the control of locomotion," Front. Comput. Neurosci., vol. 7, no. 71, 2013, doi: 10.3389/fncom.2013.00071.